

# **Investigation of blood flow as third order non-Newtonian fluid inside a porous artery in the presence of a magnetic field by an analytical method**

**Mehran Khaki Jamei<sup>1</sup>, Mohammadreza Sijani<sup>2</sup>**

Received: 26 September 2017      Accepted: 24 November 2017

**Abstract:** In this research various nonlinear fluid models have been introduced and the balloon movement in the porous arteries, including third-order non-Newtonian fluid, is described under the influence of the magnetic field. In order to solve the nonlinear equations governing the desired artery, an analytical method of approximation collocation and least squares are proposed. The effect of various parameters such as Brownian motion, thermophoresis and pressure gradient are shown on the distribution of velocity and fluid temperature. According to the studies, Increase the thermophoresis parameter and Brownian motion are increases the temperature. Also, by increasing the values of the electromagnetic parameter, fluid velocity decreases. Although many papers have investigated the flow of intra-arterial blood in the presence of MHD, it is clear that the governing equations of these articles unfortunately reveal obvious errors by extracting the governing equations. In this paper, the equations have been revised and corrected. It can also be seen by increasing the thermophoresis and Brownian parameters, increases the temperature of the nanofluid, but reduces velocity of the nanofluid and also increase the porosity parameter, the velocity of fluid flow between the balloon and the vessel wall decreases.

**Keywords:** Non-Newtonian fluid; Porous artery; Magnetic field; Thermophoresis force.

## **1. Introduction**

One of the most important causes of cardiovascular disease is blockage of the coronary arteries of the heart caused by the accumulation of cholesterol fat in the inner wall of the arteries and prevents blood flow

Gradual enlargement of the plaques increases the severity of the disease gradually. Coronary angioplasty or coronary artery bypass graft surgery is a method used to open the closed arteries of the heart. In angioplasty a small balloon is placed temporarily in the closed

---

\*. Corresponding Author:

region of the artery to help widen it. In many modern technologies and industries fluids do not follow the linear relationship between stress and strain at any point. Such fluids are referred to as non-ionic fluids. Non-native fluid flows occur in a variety of applications such as oil and gas drilling materials from industrial processes including synthetic fibers food stuffs molten plastic extrusion as well as in medicine such as intra-arterial blood flow [1-4]. Among non-Newtonian fluids viscoelastic fluid is particularly important due to the complexities of governing physical behavior and the widespread use of industrial military and medical applications. Viscoelastic fluids are a kind of non-Newtonian fluids that together have viscous and elastic properties. From the early twentieth century to now the knowledge of non-native fluid fluids (known as rheology) has been the subject of many theoretical and laboratory investigations. Agboud and Saouli [5] underwent a second-order analysis of the viscoelastic fluid on an elastic plate under the influence of the magnetic field by mass transfer and heat transfer. The effects of viscoelastic and magneto metric parameters on velocity and length as well as the effects of magneto metric parameters springs and Prandtl numbers on temperature have been investigated. It has been observed that with the increase of the viscoelastic parameter and magneto, the velocity and length decreases. By increasing the magnet and spring parameter the temperature increases and the temperature decreases with increasing Prandtl number. Hayat and Abbas [6] analyzed the heat transfer on the second-order fluid flow in a porous medium channel. In order to obtain the field of velocity and temperature an

analytical Homotopy method has been used. The results show that with increasing porosity parameter and Hartmann, number the field of velocity and temperature decreases. Hayat et al. [7] The Board and colleagues solved an analytical solution for the third-order fluid flow in a porous channel. Using the analytic Homotopy method we studied the effects of Reynolds number and Hartmann number. The results show that the analytical Homotopy method is a very effective, easy and accurate method and has a good convergence for non-niche issues. Sajid et al. [8] used a numerical method of finite element to study the third-order fluid flow on a horizontal plate with a slip condition. Their results showed that the suction speed and slip parameter play a crucial role in controlling the thickness of the boundary layer. Ellahi and Riaz [9] analyzed the effect of magnetism on the third-order fluid on the flow inside the tube with variable viscosity. Their results showed that decreasing the speed and temperature by decreasing the third-order fluid parameter and increasing the magneto metric parameter. Anjali and Ganga [10] analyzed the magnetic field hydrodynamics with heat transfer in the porous medium on an elastic surface taking into account the effects of jell and viscous heat loss. The effects of various parameters such as suction parameter, Prandtl number, magnetic parameter, temperature distribution and shell coefficient of friction in the wall have been investigated. The results show that the magnetic parameter in both longitudinal and transverse dimensions is considerably reduced. When there is porous wall there is a significant increase in temperature. By increasing the suction and Prandtl number,

the temperature decreases. As the number of ix tract increases the thickness of the magnetic boundary layer decreases. The suction and magnetic parameters reduce the frictional coefficient of the skin's wall. Agboud and Saouli [11] developed an entropy analysis for viscoelastic flow on an elastic plate. Also the effects of magneto metric parameters, springs and Prandtl numbers on speed and temperature have been investigated. The generated entropy number increases with increasing Prandtl number, magnetic parameter, surface temperature and Reynolds number. Mamaloukas et al. [12] studied the effects of the cross-magnetic magnetic field on the Maxwell fluid model on an elastic surface. To solve the equation the fourth order Runge-Kutta method was used. Examples of elastic parameter effects and magnetism parameters on velocity. The results show that by increasing the magneto metric parameter, the velocity increases and decreases with increasing elastic parameter. Ellahi et al. [13] the effects of slip on nonlinear currents of a third order non-ionic fluid were investigated between two center cylinders. It was concluded that by increasing the atmospheric pressure gauge the velocity slip increases the pressure and barometric pressure of the pressure gradient but decreases with increasing the third-order fluid flow parameter. Hatami et al. [14] simulated the transfer of gold nanoparticles in the blood

(third order non-genomic fluid) under the influence of the electromagnetic field in the porous veins. It is shown that the increase of the thermophoresis parameter increases the temperature profile, also decreases with the increase of the electromagnetic parameter of the fluid velocity profile.

According to investigations conducted by the aforementioned researchers, In this research, we try to consider the motion of an intravenous balloon with blood clots using the analytical method by considering the blood as a third order non-Newtonian fluid and also applying a magnetic field. Also, by extraction of equations in the next section, it has been determined that all articles [14-17] have obvious errors in the definition of some parameters. Unfortunately, some parameters are mistakenly removed from the equations that have been modified in the present paper.

## **2. Problem description and governing equations**

The flow of calm stable and incompressible blood is considered in the bloodstream. Blood is considered as a third-order non-Newtonian nanofluid. Base fluid nanoparticles are hydrodynamic and thermal equilibrium. Also, nanoparticles have the same size and shape. The geometry and coordinate system of the problem are shown in Fig. (1).

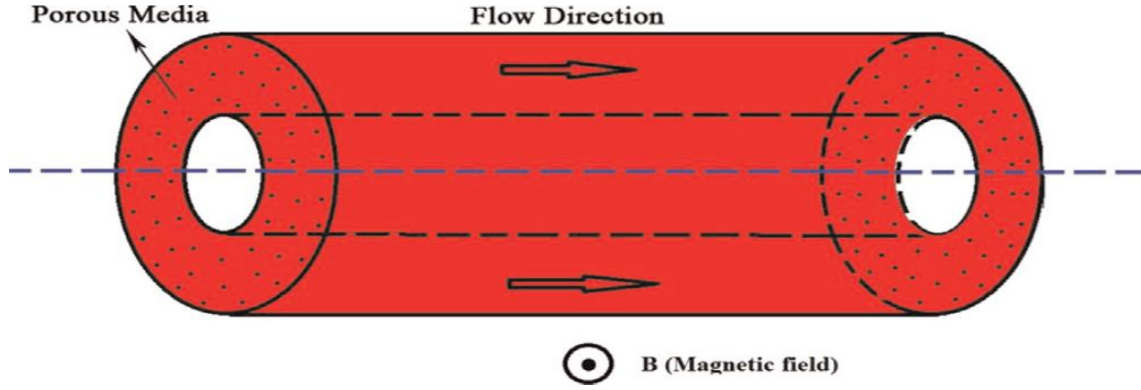


Fig 1. Schematic blood flow inside a porous artery in the presence of a magnetic field

It is assumed that the balloon is moving in the vessel at a constant speed and the space between the balloon and the vessel is porous due to artery obstruction. The fluid is an electric conductor under the influence of a  $\beta_0$  uniform magnetic field. The effects of

thermal emission of nanoparticles and Brownian motion are also considered in the transfer equations. Given the above assumptions, the mass, momentum, and energy and concentration equations are as follows [15]:

$$\rho_f \left( \frac{\partial \vec{V}}{\partial t} + \vec{V} \cdot \nabla \vec{V} \right) = \text{div} \bar{T} - \frac{\mu \phi}{k} \left( 1 + \lambda_r \frac{\partial}{\partial t} \right) \vec{V} + \rho g + \vec{J} \times \vec{B}_0 \quad (1)$$

$$(\rho c)_f \left( \frac{\partial T}{\partial t} + \vec{V} \cdot \nabla T \right) = K \nabla^2 T + (\rho c)_p \left[ D_b \nabla \phi \cdot \nabla T + \frac{D_t}{T_w} \nabla T \cdot \nabla T \right] \quad (2)$$

$$\left( \frac{\partial \phi}{\partial t} + \vec{V} \cdot \nabla \phi \right) = D_b \nabla^2 \phi + \frac{D_T}{T_w} \nabla^2 T \quad (3)$$

In the above equations  $\vec{V}$  is the velocity vector and,  $T$  temperature,  $\phi$  Concentration of nanoparticles,  $\bar{T}$  Stress tensor,  $(\rho c)_p$  heat capacity of nanoparticles,  $(\rho c)_f$  Base fluid

heat capacity,  $D_b$  Brownian diffusion coefficient,  $D_T$  thermal emission coefficients. Also  $\rho$  nanofluids density that meets the following equation [18]:

$$\rho = \phi \rho_p + (1 - \phi) \rho_f [1 - \beta_T (T - T_w)] \quad (4)$$

$\mu$  The nanofluid viscosity is considered as a function of temperature according to the Vogel's model [16]. This model has a higher accuracy than the fixed viscosity model:

$$\mu = \mu_0 e^{\left( \frac{H}{Y + \theta} - \theta_0 \right)} \quad (5)$$

$\vec{B}_0$  Is the magnetic field and  $\vec{J}$  is the current density that follows Ohm's law [19].

$$\vec{J} \times \vec{B} = -\sigma B_0^2 \vec{V} \quad (6)$$

That  $\sigma$  is the conductivity of the nanofluid. Here, it is assumed that the balloons with radius  $R$  at constant velocity

$V_0$  and the temperature  $T_0$  in the vessel move with the radius  $2R$  and the concentration of the nanoparticles is on the wall of the balloon  $\phi_w$ .

As a result, boundary conditions depend on the equations of velocity, temperature and concentration as follows:

$$\begin{aligned} r = R &\Rightarrow V = V_0, \quad T = T_0, \quad \phi = \phi_0 \\ r = 2R &\Rightarrow V = 0, \quad T = T_w, \quad \phi = \phi_w \end{aligned} \quad (7)$$

The stress tensor for a third order fluid is defined as:

$$T = -pI + \mu A_1 + \alpha_1 A_2 + \alpha_2 A_1^2 + \beta_3 (tr(A_1)) A_1 \quad (8)$$

That  $-pI$  is part of the stress due to the constraints due to the incompressibility.  $\mu$  Is the shear adhesion constant and  $a_1, a_2, b_3$  are the constants of the material. And  $A_1, A_2$  tensors are defined as follows:

$$\begin{aligned} A_1 &= (\nabla V) + (\nabla V)^t \\ A_2 &= \dot{A}_1 + A_1(\nabla V) + (\nabla V)^t A_1 \end{aligned} \quad (9)$$

The following dimensionless parameters are defined as follows:

$$\bar{V} = \frac{V}{V_0}, \bar{r} = \frac{r}{R}, \bar{\mu} = \frac{\mu}{\mu_0}, \bar{\theta} = \frac{T - T_w}{T_0 - \theta_w}, \bar{\phi} = \frac{\phi - \phi_w}{\phi_0 - \phi_w} \quad (10)$$

By substituting high dimensionless parameters in Equation (1) to (3) and simplify the governing equations are reduced:

$$\begin{aligned} \frac{d\mu}{dr} \frac{dV}{dr} + \frac{\mu}{r} \frac{dV}{dr} + \mu \frac{d^2V}{dr^2} + \frac{A}{r} \left(\frac{dV}{dr}\right)^3 + 3A \left(\frac{dV}{dr}\right)^2 \frac{d^2V}{dr^2} \\ = P\mu V + M^2V + C - Br\phi + Gr\theta - G_t\phi\theta - B_t \end{aligned} \quad (11)$$

$$N_b \frac{\partial \theta}{\partial r} \frac{\partial \phi}{\partial r} + \frac{1}{r} \frac{\partial \theta}{\partial r} + \frac{\partial^2 \theta}{\partial r^2} + N_t \left(\frac{\partial \theta}{\partial r}\right)^2 = 0 \quad (12)$$

$$N_b \left(\frac{\partial^2 \phi}{\partial r^2} + \frac{1}{r} \frac{\partial \phi}{\partial r}\right) + N_t \left(\frac{\partial^2 \theta}{\partial r^2} + \frac{1}{r} \frac{\partial \theta}{\partial r}\right) = 0 \quad (13)$$

In the above equations  $P$  Porosity parameters,  $M$  Magnetic parameters,  $A$  third order fluid flow parameter,  $C$  Pressure gradient parameter,  $N_t$  thermophoresis

Parameter,  $N_b$  Brownian parameter,  $Br$  Brownian diffusion parameters,  $Gr$  Grashof number, And  $B_t, G_t$  constant coefficients are given as follows:

$$\begin{aligned}
A &= \frac{2\beta_3 V_0^2}{\mu_0 R^2}, C = \frac{\left(\frac{\partial \hat{P}}{\partial Z}\right) R^2}{V_0 \mu_0}, P = \frac{\varphi R^2}{K}, M^2 = \frac{G_0 B_0^2 R^2}{\mu_0} \\
Br &= \frac{(\rho_p - \rho_f) R^2 (\phi_m - \phi_w) g}{\mu_0 V_0}, Gr = \frac{(\theta_m - \theta_w) \rho_f R^2 \beta_T (1 - \phi_w) g}{\mu_0 V_0} \\
Bt &= \frac{(\rho_f (1 - \phi_w) + \rho_f \phi_w) R^2 g}{\mu_0 V_0}, Gt = \frac{\rho_f (\phi_m - \phi_w) R^2 (\theta_m - \theta_w) \beta_T g}{\mu_0 V_0}
\end{aligned} \tag{14}$$

The boundless boundary conditions for equations (11) to (13) are obtained as follows:

$$\begin{aligned}
r = 1 &\Rightarrow V = V_0, \quad \theta = 1, \quad \phi = 1 \\
r = 2 &\Rightarrow V = 0, \quad \theta = 0, \quad \phi = 0
\end{aligned} \tag{15}$$

It is clear from the extraction of equations that, unfortunately, in all papers [14-17], Fields  $N_t$  and  $N_b$  are incorrectly changed in equation (13) and sentences that affect the parameters of  $Gt$  and  $Bt$  are erroneously deleted in all of these papers And their effect is ignored. The main purpose of this paper is to solve this problem with the corrected governing equations, which is presented in the next section.

### 3. Collocation (CM) and Least Squares (LSM)

One of the approximate analytical methods for solving differential equations is the Weighted Residual Methods (WRMs). In the WRMs, the weight functions are those functions that are arbitrarily selected and used in this method. But the type of arbitrary functions that can be used can affect the solution. The WRMs is classified according to the type of weighting function used in different ways. These methods can be summarized as follows: Collocation method, Galerkin method, Least squares method. In this paper used the collocation and least

squares method to solve the problem. Suppose we have the following differential equation:

$$D(u(x)) = p(x) \tag{16}$$

The answer to this differential equation (the estimation function) is assumed to be a linear combination of arbitrary functions (base functions):

$$u = \tilde{u} = \sum_{i=1}^n c_i \varphi_i \tag{17}$$

The placement of the estimated function within the differential equation gives us the remainder or the error:

$$E(x) = R(x) = D(\tilde{u}(x) - p(x)) \neq 0 \tag{18}$$

Now the Dirac Delta function is defined according to its effect on other functions as follows:

$$\int_{-\infty}^{+\infty} \delta(x) dx = 1 \tag{19}$$

The consequences of this definition are as follows:

$$\int_{\Omega} \delta(x - \xi) f(x) dx = \begin{cases} f(\xi) & \xi \in \Omega \\ 0 & \xi \notin \Omega \end{cases} \tag{20}$$

In the collocation method we use the property defined for the Dirac delta function Equation (20). Thus, we consider the weighted functions used in Dirac's delta functions  $\delta(x - x_i)$  that  $x_i$  as arbitrary point

coordinates within the definition of the differential equation. It is obvious that the number of unknown coefficients in the estimation function is considered to be a point. In this case we will have (if the point is needed, in other words, the unknown coefficient in the function is estimated:

$$\begin{aligned}
 \int_{\Omega} \delta(x - x_1) R(x) dx &= 0 \\
 \int_{\Omega} \delta(x - x_2) R(x) dx &= 0 \\
 \int_{\Omega} \delta(x - x_3) R(x) dx &= 0 \\
 \vdots \\
 \int_{\Omega} \delta(x - x_n) R(x) dx &= 0
 \end{aligned} \tag{21}$$

In this way, there are three independent equations that can be used to obtain the unknown coefficients of the estimation function.

In some cases, we need to obtain the best and most optimal estimation function for the differential equation. To do this, we need to get the estimated function with the minimum error in the range. In this case, the integral above represents the sum of the sum of the remaining squares or the same errors within the definition of the differential equation. In order to obtain the optimal response, the coefficients of the base functions must be obtained in such a way that the sum of the squares of the errors is minimal. To do this, we deduce from the sum of the squares of errors the differential of each of the coefficients of the basic functions and make it equal to zero. In other words, we minimize the sum of squares of errors compared to the basic function coefficients. This method is known as the least squares (LSM) method.

$$\frac{d}{dc_i} \int_{\Omega} R^2 dx = 0 \tag{22}$$

#### 4. Results

The nonlinear differential equations (11) to (13) with respect to boundary conditions (15) are analyzed analytically using the residual weight method and numerically using the Runge-Kutta method for different values of porosity parameters, magnet parameter, third order fluid parameter, pressure gradient parameter, thermophoresis parameter, Brownian parameter and Brownian diffusion parameter are solved. In order to validate the results of the present study, the results were first compared to the distribution of velocity, temperature and concentration of the collocation method with the analytical results obtained from reference [15] in Figures (2- 4).

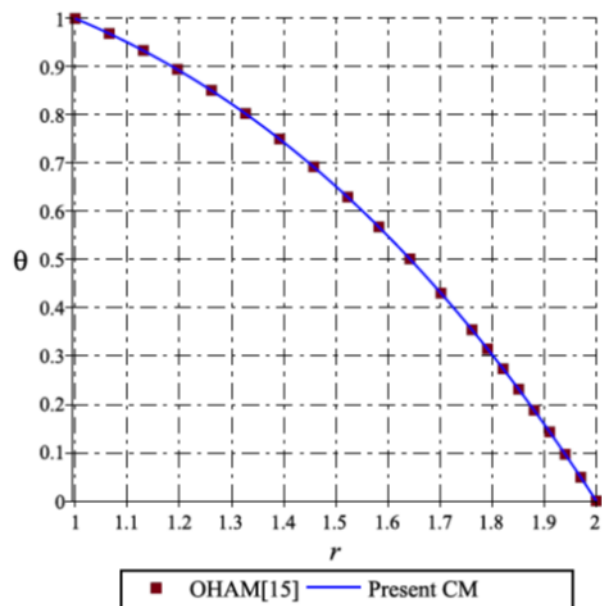


Fig2. temperature comparison diagram with CM in this research and OHAM Reference [15]

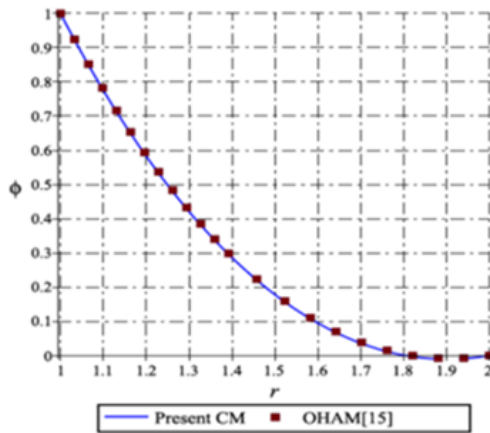


Fig3. Concentration comparison diagram with CM in this research and OHAM Reference [15]

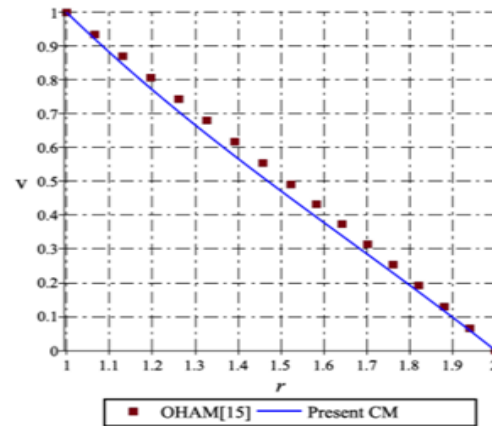


Fig4. Velocity comparison diagram with CM in this research and OHAM Reference [15]

In the case of considering all the parameters, one corresponds to all the graphs. Also Figures (5-7)

show the comparison of collocation and least squares methods with numerical results.

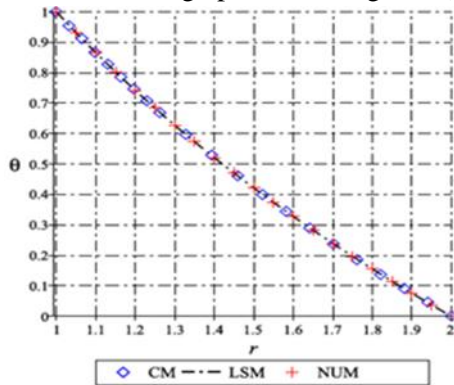


Fig5. Validation diagram and accuracy of temperature distribution in the collocation and least square method with numerical method

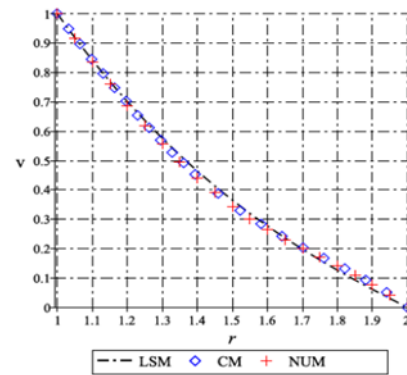


Fig7. Validation diagram and accuracy of velocity distribution in the collocation and least square method with numerical method

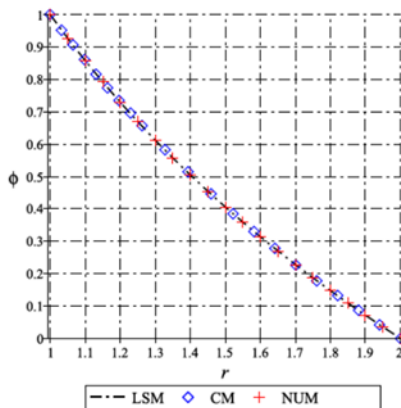


Fig6. Validation diagram and accuracy of concentration distribution in the collocation and least square method with numerical method

The numerical values of these methods and their errors are shown in tables (1) to (3) for different values. Given the shapes and tables, a good match is observed in all modes.

**Table1.***Comparison of CM and LSM with Numerical method for  $\theta$* 

$r$	CM	LSM	NUM	error CM	error LSM
1	1	1	1	0	0
1.1	0.8655360185	0.8652995783	0.8654433988	9.26197E-05	0.00014382
1.2	0.7418783125	0.7414742248	0.7417924427	8.58698E-05	0.000318218
1.3	0.6274312719	0.6270291904	0.6273571958	7.40761E-05	0.000328005
1.4	0.5208872313	0.5206458976	0.5208160218	7.12095E-05	0.000170124
1.5	0.4211842544	0.4211819407	0.4211153207	6.89337E-05	6.662E-05
1.6	0.3274639244	0.3276710853	0.3274013019	6.26225E-05	0.000269783
1.7	0.2390291309	0.2393232689	0.2389722258	5.69051E-05	0.000351043
1.8	0.1553018576	0.1555246003	0.1552441497	5.77079E-05	0.000280451
1.9	0.07578096904	0.07583735998	0.07572583184	5.51372E-05	0.000111528
2	0	0	0	0	0

**Table2.***Comparison of CM and LSM with Numerical method for  $\phi$* 

$r$	CM	LSM	NUM	error CM	error LSM
1	1	1	1	0	0
1.1	0.8582097363	0.8578786525	0.8580760923	0.000134	0.0002
1.2	0.7298484092	0.7292867568	0.7297253212	0.000123	0.00044
1.3	0.6127909499	0.6122386863	0.6126851481	0.000106	0.00045
1.4	0.5053106129	0.5049900686	0.5052088993	0.000102	0.00022
1.5	0.4060192989	0.4060377850	0.4059207670	9.85E-05	0.000117
1.6	0.3138078724	0.3141199708	0.3137182843	8.96E-05	0.000402
1.7	0.2277864811	0.2282160153	0.2277047953	8.17E-05	0.000511
1.8	0.1472248786	0.1475465613	0.1471415090	8.34E-05	0.000405
1.9	0.0714927439	0.0715735060	0.07141270584	8E-05	0.000161
2	0	0	0	0	0

**Table3.***Comparison of CM and LSM with Numerical method for  $V$* 

$r$	CM	LSM	NUM	error CM	error LSM
1	1	1	1	0	0
1.1	0.8439925399	0.8419232023	0.8360301206	0.007962	0.005893
1.2	0.695816287	0.7010451712	0.6874328538	0.008383	0.013612
1.3	0.561966417	0.5757561022	0.5553183575	0.006648	0.020438
1.4	0.446215488	0.4644461912	0.4406129683	0.005603	0.023833
1.5	0.349613427	0.3655056338	0.3438245520	0.005789	0.021681
1.6	0.270487542	0.2773246257	0.2643925332	0.006095	0.012932
1.7	0.204442510	0.1982933625	0.1992519811	0.005191	0.00096
1.8	0.144360394	0.1268020401	0.1409353083	0.003425	0.01413
1.9	0.080400620	0.06124085394	0.07800076019	0.0024	0.01676
2	0	0	0	0	0

Figs (8), (9) and (10) show the effect of the thermophoresis parameter on the distribution of temperature, concentration and velocity. It is observed that with increasing thermophoresis parameters the temperature increases. Also, according to Figs. (9) and (10), it is clearly observed that with the increase of the thermophoresis parameter, the concentration and velocity of nanofluid decreases.

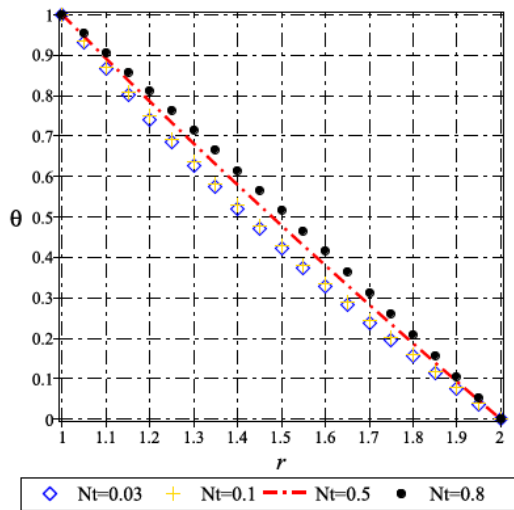


Fig8. Effect of Thermophoresis parameter on temperature profile

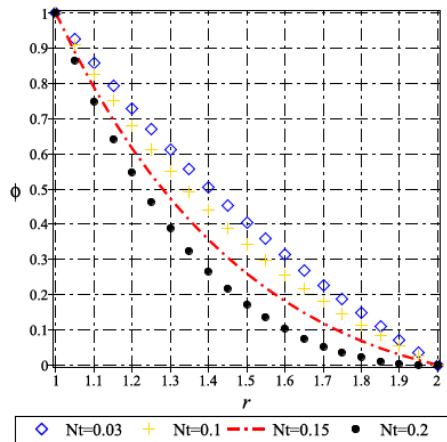


Fig9. Effect of Thermophoresis parameter on nanoparticles concentration profile

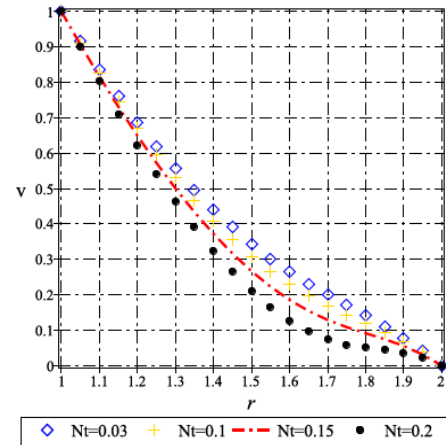


Fig10. Effect of Thermophoresis parameter on velocity profile

The effect of Brownian motion on the temperature, concentration and velocity distribution is shown in Figures (11-13). By increasing the Brownian parameter, such as the thermophoresis parameter, the temperature of the nanofluid increases (Fig. 11) but as the parameter increases, the velocity decreases (Fig. 12) It is also seen in (Fig. 13) that the Brownian parameter has no effect on the concentration of the nanoparticle.

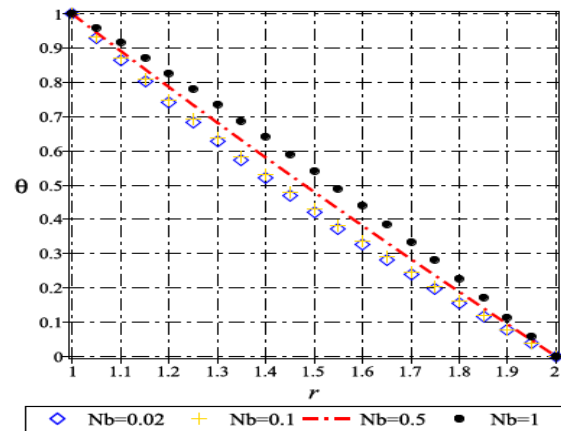


Fig11. Effect of Brownian motion parameter on temperature profile.

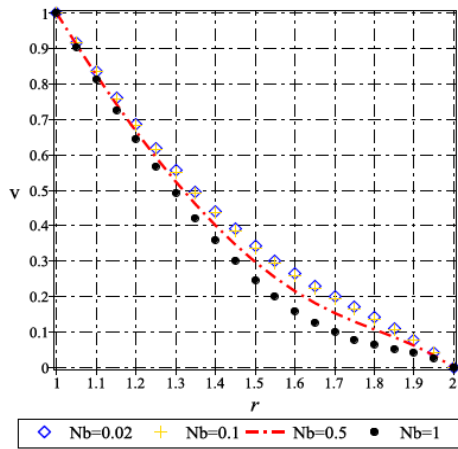


Fig12. Effect of Brownian motion parameter on velocity profile.

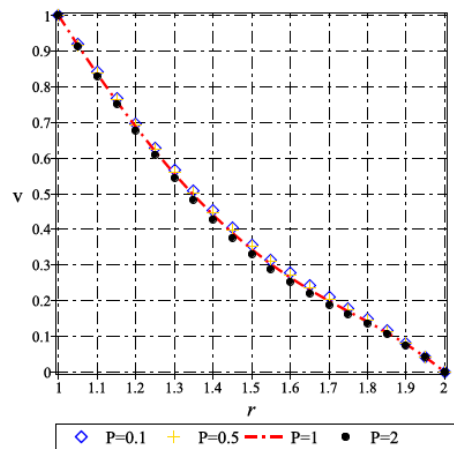


Fig14. Effect of porosity parameter on velocity profile.

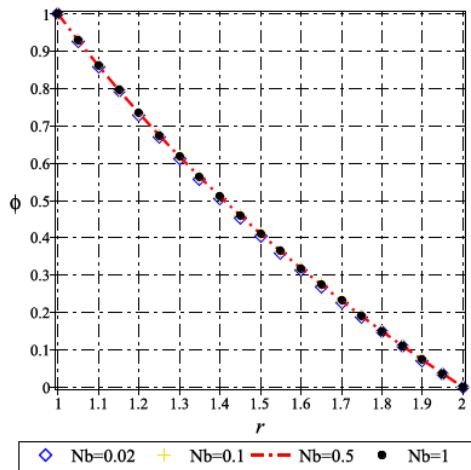


Fig13. Effect of Brownian motion parameter on nanoparticle concentration profile.

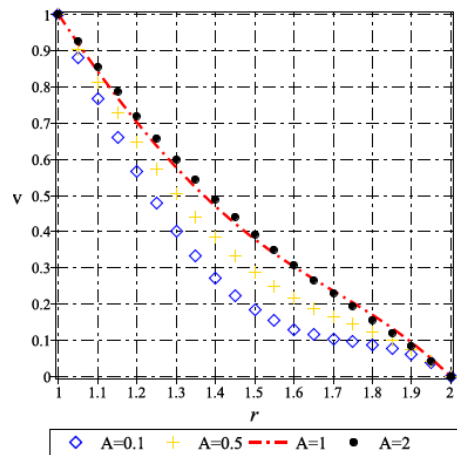


Fig15. Effect of third-grade parameter on velocity profile.

Figure (14-17) shows the effect of porosity, non-Newtonian fluid parameter, magnetic field and pressure gradient on the nanofluid velocity distribution. With increasing porosity and gradient of pressure, the velocity increases which is obvious but decreases with increasing magnetic field. Because this parameter generates Lorentz force and this friction creates friction against the direction of flow and reduces the velocity.

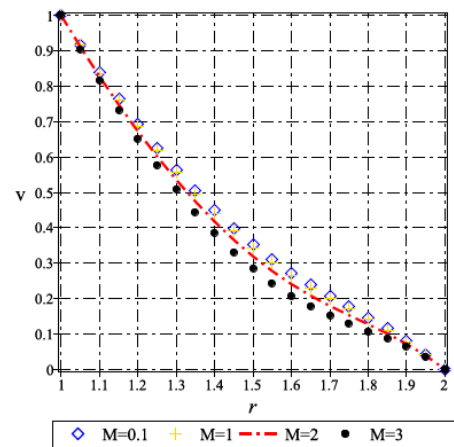


Fig16. Effect of MHD parameter on velocity profile.

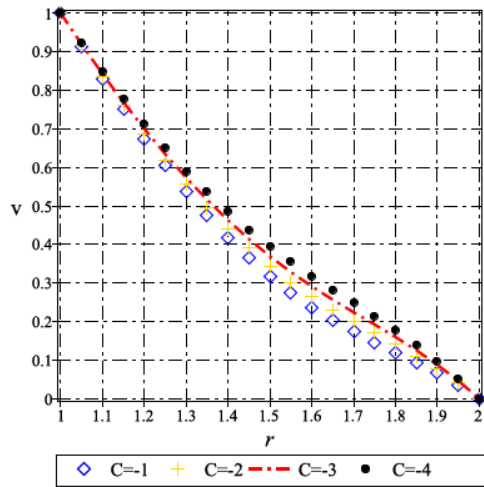


Fig17. Effect of pressure gradient on velocity profile.

## 5. Discussion

The recent studies of [14-17] is improved in this paper considering the effects of the parameters of  $Gt$  and  $Bt$  on governing equation, thus, not restricted to the cases  $Gt = 0$  and  $Bt = 0$  of [14-17]. Also the results indicate that the temperature distribution is strongly depending on the thermophoresis and Brownian numbers.

Finally, it is worthy to mention that the analytical solutions presented in this paper may provide insight into the physical phenomena of the problem at hand and also they could be used as benchmarks or validation tests for the numerical schemes. these methods solve the equations directly and do not need any perturbation, linearization, simplifications or small parameter versus Homotopy Perturbation Method (HPM) and Parameter Perturbation Method (PPM).

## 6. Conclusion

In this research, by applying the method of collocation (CM) and least squares (LSM), with effect of different parameters on the distribution of velocity temperature and concentration of nanofluid in the porous artery in the presence of a magnetic field has been investigated. According to the studies, the following results are obtained:

1. With increasing thermophoresis parameters, increases the temperature of the nanofluid if the parameter increases, the velocity and concentration of the nanofluid are reduced.
2. With Increasing the Brownian parameter increases the temperature of the nanofluid but this parameter does not have any effect on concentration, but reduces velocity.
3. If the porosity parameter is increased, the flow velocity decreases between the balloon and the wall of the vein.
4. If the MHD parameter is increased, decreases the flow velocity between the balloon and the wall of the vein.
5. If the third-order non-Newtonian parameter is increased, increases the flow velocity between the balloon and the wall of the vein.

**Nomenclature:**

Stress tensor	$T$
velocity	$V$
Dimensionless number Brownian	$Br$
Viscosity constants	$H, Y$
Pressure gradient	$C$
Brownian diffusion coefficient	$D_b$
Thermophoresis coefficient	$D_T$
Electrical Field	$E$
Acceleration of gravity	$g$
Grashov number	$Gr$
Electrical current density	$J$
Parameter MHD	$M$
Porosity parameter	$P$
Permeability	$K$
Thermophoretic parameter	$N_t$
Braun parameter	$N_b$
Variable radius	$r$
Radiation of arteries	$R$
Reference speed	$V_0$
The modules of matter	$\alpha, \beta$
Coefficient of thermal expansion	$\beta_T$
Third order non-Newtonian parameter	$A$
Time lag	$\lambda_r$
Viscosity	$\mu$
Reference viscosity	$\mu_0$
Volume fraction	$\phi$
Volume fraction of the inner wall	$\phi_m$
Volume fraction of the external wall	$\phi_w$
Temperature	$\theta$
Internal wall temperature	$\theta_m$
External wall temperature	$\theta_w$
Base fluid density	$\rho_f$
Density of the nanoparticle	$\rho_p$
Porosity	$\varphi$
Electrical conductivity	$\sigma$
Dimensionless parameter	$Gt$
Dimensionless parameter	$Bt$

**References**

[1] H.E. Abdel Baieth, Physical parameters of blood as a non-Newtonian fluid, International Journal of Biomedical Science 4.4 (2008) 323–329.  
 [2] I. Rahimi Petroudi, Analytical solution of Non-Newtonian fluid flow in permeable channel, MSc. Thesis,

Islamic Azad University Sari branch. 120 (2013) 4–19.  
 [3] T. Hayat, N. Ahmed, M. Sajid, S. Asghar, On the MHD flow of a second grade fluid in a porous channel, Computers and Mathematics with Applications. 54 (2007) 407–414.  
 [4] S. Dinarvand, A. Doosthoseini, E. Doosthoseini, M. M. Rashidi, Comparison of HAM and HPM methods for Berman’s model of two-dimensional viscous flow in porous channel with wall suction or injection, Advances in Theoretical and Applied Mechanics 1 (2008) 337–347.  
 [5] S. Agboud, S. Saouli, Second law analysis of viscoelastic fluid over a stretching sheet subject to a transverse magnetic field with heat and mass transfer, Entropy. 12 (2010) 1867-1884.  
 [6] T. Hayat, Z. Abbas, Heat transfer analysis on the MHD flow of a second Grade fluid in a channel with porous medium, Chaos, Solitons and Fractals. 38 (2008) 556–567.  
 [7] T. Hayata, N. Ahmeda, M. Sajidb, Analytic solution for MHD flow of a third order fluid in a porous channel, Journal of Computational and Applied Mathematics. 214 (2008) 572–582.  
 [8] M. Sajid, R. Mahmood, T. Hayat, Finite element solution for flow of a third grade fluid past a horizontal porous plate with partial slip, Computers and Mathematics with Applications. 56 (2008) 1236-1244.  
 [9] R. Ellahi, A. Riaz, “Analytical solutions for MHD flow in a third-grade fluid with variable viscosity”, Mathematical and Computer Modelling. 52 (2010) 1783-1793.

- [10] S.P. A. Devi, B. Ganga, Dissipation effects on MHD nonlinear flow and heat transfer past a porous surface with prescribed heat flux, *Journal of Applied Fluid Mechanics*. 3 (2009) 16.
- [11] S. Agboud, S. Saouli, Entropy analysis for viscoelastic magnetohydrodynamic flow over a stretching surface, *International Journal of Non-Linear Mechanics*. 45 (2010) 482–489.
- [12] Ch. Mamaloukas, M. Subhas Abel, J.V. Tawade, U.S. Mahabaleswar, on effects of a transverse magnetic field on an UCM fluid over a stretching sheet, *International Journal of Pure and Applied Mathematics*. 661 (2011) 1-9.
- [13] R. Ellahi, T. Hayat, F.M. Mahomed, S. Asghar, Effects of slip on the non-linear flows of a third grade fluid, *Nonlinear Analysis: Real World Applications*. 11 (2010) 139-146.
- [14] M. Hatami, J. Hatami, D.D. Ganji, Computer simulation of MHD blood conveying goldnanoparticles as a third grade non-Newtonian nanofluid in a hollow porous vessel, computer methods and programs in biomedicine. 113 (2014) 632–641.
- [15] S. E. Ghasemi, M. Hatami, A. Kalani Sarokolaie, D.D. Gnaji, Study on blood flow containing nanoparticles through porous arteries in presence of magnetic field using analytical methods. *Physica E: Low-dimensional Systems and Nanostructures* 70 (2015) 146-156.
- [16] R. Ellahi, M. Raza, K. Vafai, Series solutions of non-Newtonian Nano fluids with Reynold's model and Vogel's model by means of the homotopy analysis method, *Mathematical and Computer Modelling* 55 (2012) 1876–1891.
- [17] R. Ellahi, A. Zeeshan, K. Vafai, H.U. Rahman, Series solutions for magneto hydrodynamic flow of non-Newtonian Nano fluid and heat transfer in coaxial porous cylinder with slip conditions, *Journal of Nanoengineering and Nanosystems* 225 (2011) 123–132.
- [18] D. Yadav, G.S. Agrawal, R. Bhargava, Thermal instability of rotating Nano fluid layer, *International Journal of Engineering Science* 49 (2011) 1171-1184.
- [19] S. Asghar, K. Hanif, T. Hayat, C.M. Khaliq, MHD non-Newtonian flow due to non-co axial rotations of an accelerated disk and a fluid at infinity, *Communications in Nonlinear Science and Numerical Simulation* 12.4 (2007) 465-485.